The circadian system alters thermoregulation depending on the time of day and feeding condition

Ken Tokizawa[1)], Yuki Uchida[1)] and Kei Nagashima[1),2)]

[1)] Laboratory of Integrative Physiology, Faculty of Human Sciences, and [2)] Consolidated Research Institute for Advanced Science and Medical Care, Waseda University, 2-579-15Mikajima, Tokorozawa, Saitama, 359-1192, JAPAN

Corresponding Author: Kei Nagashima, MD

Laboratory of Integrative Physiology

Faculty of Human Sciences, Waseda University

Mikajima 2-579-15, Tokorozawa, Saitama, 359-1192, Japan

Tel & Fax: +81-4-2947-6918

Email: k-nagashima@waseda.jp

Abstract

The circadian rhythm of body temperature (T_b) is a well-known phenomenon. However, it is unknown how the circadian system affects thermoregulation. Food deprivation in mice induces a greater reduction of T_b particularly in the light phase. We examined the role of the clock gene and the suprachiasmatic nucleus (SCN) during induced hypothermia. At 20°C with fasting, mice increased their metabolic heat production in the dark phase and maintained T_b, whereas in the light phase, heat production was less, resulting in hypothermia. Under these conditions, neuronal activity in the SCN, assessed by cFos expression, increased only in the light phase. The differences between the phases in *Clock* mutant mice were less marked. The neural network between the SCN and paraventricular nucleus appeared to be important in hypothermia. These findings suggest that the circadian system per se is influenced by both the feeding condition and environmental temperature and that it modulates thermoregulation.

Homeostasis is the goal of various physiological responses in animals. Many physiological parameters show a circadian oscillation or rhythm. Body temperature (T_b) in homeothermic animals has a circadian rhythm[1]. Despite the discovery of clock genes and their expression mechanisms[2], little is known about the mechanisms involved in the generation of the T_b rhythm or its physiological significance.

Homeotherms regulate their T_b, by controlling the balance between heat production and heat loss. The circadian T_b rhythm appears to be regulated by these mechanisms. Our preliminary results indicated that the T_b rhythm is maintained through the modulation of heat loss in both warm and cool environments (unpublished data). However, there are anomalies in the homeostasis of the T_b rhythm. Laboratory mice and rats decrease their T_b with decreases in caloric availability, although the reduction is smaller than in hibernators during torpor when T_b is less than 20°C[3]. This torpor-like hypothermia in mice and rats appears to be controlled by the circadian system because fasting rats reduce T_b more in the inactive phase than in the active phase [4–6]. Ablation of the suprachiasmatic nucleus (SCN), the master circadian clock, abolishes T_b reduction during fasting[7]. These findings suggest that the torpor-like hypothermia is not the result of the disruption of the homeostasis of the T_b rhythm but is regulated and controlled by the SCN.

Nagashima et al.[6] reported that metabolic heat production in rats greatly decreased throughout a day of fasting. T_b was maintained by suppressing heat loss. However, heat loss suppression was observed only in the dark phase (active phase), which resulted in maintained T_b in the dark phase and torpor-like hypothermia in the light phase. They also reported that in double-knockout mice (*Cry*1 and *Cry*2, the key clock genes), metabolic heat production determined T_b in both ad-lib feeding and fasting conditions[8]. However, in wild-type mice, T_b was higher in the active phase

than in the inactive phase at a given level of heat production, indicating a change in the heat-loss response. Thus, thermoregulatory responses are different under ad-lib feeding and fasting conditions and are different in active and inactive phases, in which clock genes may be involved.

We tested the hypothesis that modulation of thermoregulatory responses by the circadian system (including the SCN and clock genes) depends on the time of day and feeding condition. We compared the physiological and neural responses during exposure to cold at 20°C under ad-lib feeding and fasting conditions, and in dark and light phases. Differences in these responses between normal and *Clock* mutant mice were also examined. *Clock* is one of the genes organizing the core loop of molecular circadian oscillation. The mutation of *Clock* results in a disappearance of the oscillation[9]. However, mutant mice show a T_b rhythm under light-dark condition because of a masking effect of lighting. We measured T_b, metabolic heat production, and uncoupling protein-1 (UCP1) mRNA in interscapular brown adipose tissue (iBAT). We also determined cFos expression (reflecting neural activity) in the SCN and other hypothalamic areas related to thermoregulation. Our assumptions were that (1) the physiological and neuronal thermoregulatory responses to the cold would be different under different lighting and feeding conditions; (2) the SCN would be involved; and (3) *Clock* mutant mice would not show these differences in thermoregulatory responses. We traced those hypothalamic areas receiving signals from the SCN that may be involved in the modulation of thermoregulation to identify the connections between the circadian and thermoregulation systems.

RESULTS

Circadian changes in T_b, metabolism, and activity during ad-lib feeding and fasting

Figure 1 shows typical examples of the changes in T_b, oxygen consumption rate ($\dot{V}O_2$), and spontaneous activity during ad-lib feeding and fasting in wild-type and *Clock* mutant mice. With ad-lib feeding, each parameter for wild-type mice showed a clear circadian rhythm. Although there were small fluctuations in each parameter in *Clock* mutant mice, the light-linked rhythm appeared to be maintained. As previously reported, the 24-h rhythm in *Clock* mutant mice was abolished in constant darkness (data not shown). Fasting for two days reduced both T_b and $\dot{V}O_2$ in the wild-type mice. There was no change in spontaneous activity, which was greater ($P < 0.05$) in the light phase than in the dark phase, but the circadian rhythm was maintained. In *Clock* mutant mice, T_b and $\dot{V}O_2$ decreased during fasting. The change in body weight after fasting did not differ between animals starting fasting in the dark phase and light phase, or between wild-type mice and *Clock* mutant mice (–14.0 to –14.2%).

Thermoregulatory responses in the cold

The cold responses in wild-type mice. In the cold (20°C) during ad-lib feeding, T_b in the wild-type mice was similar to that at 27°C in both the dark and the light phases (**Fig. 2a,b**). However, $\dot{V}O_2$ was greater than at 27°C only in the light phase (ZT2.5–3.5, **Fig. 2e**). In the cold during fasting, the reduction in T_b increased in both the light and the dark phases (ZT1–4 and 14.5–16, respectively; **Fig. 2a,b**), but the decrease was much larger ($P < 0.05$) in the light phase (**Fig. 2i**). $\dot{V}O_2$ increased ($P < 0.05$) at 27°C at ZT13.5–14.5 in the dark phase (**Fig. 2f**), but remained unchanged in the light phase (**Fig. 2e**). The change in $\dot{V}O_2$ in the cold during fasting was greater ($P < 0.05$) in the dark

phase than in the light phase (**Fig. 2j**). Spontaneous activity did not change in the cold during either ad-lib feeding or fasting (**Fig. 3a,b,e,f**).

The cold responses in Clock mutant mice. In the cold during ad-lib feeding, T_b in *Clock* mutant mice was maintained at the 27°C level (**Fig. 2c,d**). $\dot{V}O_2$ increased ($P < 0.05$) above the level at 27°C in both the dark and the light phases (ZT3–4 and 13.5–14; **Fig. 2g,h**) with no difference between the two phases. In the cold during fasting, T_b was lower ($P < 0.05$) than the 27°C level at ZT3–3.5 in the light phase and ZT14.5–16 in the dark phase (**Fig. 2c,d**) with no significant difference between the phases (**Fig. 2i**). $\dot{V}O_2$ was greater ($P < 0.05$) than the 27°C level at ZT2 and 13.5–14 (**Fig. 2g,h**). This increase in $\dot{V}O_2$ was greater ($P < 0.05$) in the dark phase than in the light phase (**Fig. 2j**). Spontaneous activity in the cold was greater ($P < 0.05$) than that at 27°C only in the dark phase (**Fig. 3d,h**). The reductions in T_b in *Clock* mutant mice were smaller ($P < 0.05$) than in the light phase of wild-type mice, and the increase in $\dot{V}O_2$ was greater ($P < 0.05$) than in the light phase of the wild-type mice. The changes in *Clock* mutant mice were similar to those observed in the dark phase in the wild-type mice.

UCP1 mRNA expression in the cold

UCP1 mRNA in the wild-type mice. There was no difference in wild-type mice in the level of UCP1 mRNA between the light and dark phases at 27°C during ad-lib feeding (**Fig. 4**). Cold exposure during ad-lib feeding did not affect the level of UCP1 mRNA. UCP1 mRNA during fasting decreased ($P < 0.05$) from the ad-lib feeding level only in the light phase. However, UCP1 mRNA increased in the cold ($P < 0.05$) in the dark phase; but remained unchanged in the light phase.

UCP1 mRNA in Clock mutant mice. The level of UCP1 mRNA in *Clock*

mutant mice was similar in the two phases at 27°C during ad-lib feeding. Exposure to cold at 20°C during both ad-lib feeding and fasting had no influence on levels of UCP1 mRNA, but the level was increased during fasting in both phases ($P < 0.05$) with no significant difference between the two. The increase in UCP1 mRNA in the cold was greater ($P < 0.05$) in *Clock* mutant mice than in wild-type mice in the light phase.

cFos expression in the hypothalamic areas

During ad-lib feeding, counts of cFos-immunoreactive (IR) cells were low in the medial preoptic nucleus (MPO, **Fig. 5a**), dorsomedial nucleus (DMH, **Fig. 5b**), arcuate nucleus (ARC, **Fig. 5c**), and paraventricular nucleus (PVN, **Fig. 5d**) at 27°C in both wild-type and *Clock* mutant mice. There were no significant differences in counts between the light and dark phases. In wild-type mice, counts of cFos-IR cells in the dorsal subparaventricular zone (dSPZ, **Fig. 5e**) were greater ($P < 0.05$) during the dark phase than the light phase, with the opposite pattern in the SCN (**Fig. 5f**). In *Clock* mutant mice, no significant difference between the phases was observed in the MPO, DMH, ARC, PVN, and dSPZ. The counts in the SCN were greater in the light phase than in the dark phase, but the difference was smaller than in the wild-type mice. In the dark phase during fasting, counts of cFos-IR cells in the wild-type mice increased in all areas, whereas increases were observed in the light phase only in the DMH, dSPZ, and SCN. The counts increased in *Clock* mutant mice during fasting in the DMH, ARC, and PVN in the dark phase, and the DMH, ARC, and SCN in the light phase with no significant differences between the two phases. The increases in the counts in the DMH, ARC, PVN, and dSPZ in the dark phase were smaller in *Clock* mutant mice than in wild-type mice.

cFos-IR cells in the cold in the wild-type mice. In the cold during ad-lib

feeding, counts of cFos-IR cells in the MPO were greater than those seen at 27°C only in the light phase (**Fig. 5a**). The counts were unchanged in the other hypothalamic areas in the cold. During fasting, cold increased cFos-IR cells in the MPO, DMH, PVN, and dSPZ in the dark phase, whereas all areas showed an increase in counts in the light phase. During fasting, the cold increased cFos-IR cells in the SCN only in the light phase (**Fig. 5f**).

cFos-IR cells in the cold in Clock mutant mice. Cold exposure during ad-lib feeding resulted in increases in the counts of cFos-IR cells in the MPO, DMH, and SCN only in the dark phase. The counts of cFos-IR cells in the SCN in both the dark and the light phases were less than in wild-type mice. In the cold during fasting, the counts were greater than the values at 27°C in the MPO, DMH, ARC, PVN, and dSPZ in both the dark and the light phases, with no significant difference between the two phases.

Table 1 summarized cFos expression at 20°C with fasting in the hypothalamic areas in wild-type and *Clock* mutant mice. In addition, physiological responses in the conditions were also shown.

Immunofluorecent-histochemistry for cFos, glutamate decarboxylase (GAD) 65, and cholera toxin b-subunit (CTb)

In both the wild-type and the *Clock* mutant mice, injection of CTb (monosynaptic retrograde neural tracer) in the PVN resulted in widely spread labeling in both the dorsomedial and the ventrolateral parts of the SCN, but not outside the SCN. In the wild-type mice, 5–10% of CTb-labeled neurons in the SCN were also cFos-positive at 27°C in the light phase during ad-lib feeding (**Fig. 6a,b**). In the cold during fasting, the ratio of the double-labeled neurons increased ($P < 0.05$, 25–30%; **Fig. 6c,d**). However, in *Clock* mutant mice, the double-labeled neurons remained at 5–10% in the

cold during fasting (**Fig. 6e,f**). Double-labeled neurons counted separately in the dorsomedial and ventrolateral SCN in wild-type mice showed no difference between the two areas (cFos + CTb/Total CTb, dorsomedial, 5.3/27.0; ventrolateral, 6.7/26.0). In the SCN, GAD65- (GABA synthetase) positive neurons were observed in a punctate pattern in close apposition to the double-labeled neurons (**Fig. 6g**). CTb injection in the MPO resulted in retrograde labeling in the dorsomedial parts of the SCN. In this area, the ratio of the double-labeled neurons remained at the same level both at 27°C during ad-lib feeding and at 20°C during fasting (15–20%) in wild-type mice.

DISCUSSION

We found different physiological responses in wild-type mice to the cold condition between ad-lib feeding and fasting, and between the dark and light phases. The neural responses in the hypothalamus, as shown by cFos expression, were also different. However, these differences in physiological and neural responses were absent or greatly decreased in *Clock* mutant mice. The SCN appears to be important in the changes in thermoregulatory responses. Circadian T_b rhythm is a well-known phenomenon. We do not know how the circadian system influences T_b, and the physiological significance is unclear. However, we can offer partial answers to these questions.

Effect of fasting on T_b, metabolic heat production, and neural responses in the hypothalamus

The fasting-induced reductions in T_b and $\dot{V}O_2$ throughout the day in the wild-type mice were greater in the light phase than in the dark phase (**Fig. 1a**). The reduction in T_b was augmented immediately after lights-on (ZT0–6, torpor-like hypothermia) with little change in $\dot{V}O_2$. This finding is similar to that reported in rats[6]. Because the reduction in body weight was not different between the animals starting fasting in the dark phase or light phase, the influence of energy availability on the difference in T_b appears small. The level of UCP1 mRNA showed no circadian change during ad-lib feeding and fasting in wild-type mice, although fasting induced a small reduction in the light phase (**Fig. 4**). Thus, thermogenesis in the iBAT may have contributed to the $\dot{V}O_2$ rhythm slightly during ad-lib feeding, but was not activated by fasting despite the greater reduction in T_b.

Our earlier preliminary observations showed a random, torpor-like hypothermia during constant darkness in wild-type mice, indicating that it was

influenced by light. Circadian rhythms in T_b and $\dot{V}O_2$ in *Clock* mutant mice were observed during ad-lib feeding despite small fluctuations in each phase (**Fig. 1d**). T_b and $\dot{V}O_2$ also decreased during fasting in *Clock* mutant mice, with no difference in the mean values in the light and dark phases and similar values to those during the light phase in wild-type mice (**Fig. 2a–d**). However, during fasting there was no long-lasting hypothermia as observed in wild-type mice (**Fig. 1d**). *Clock* plays an important role in the core loop of the molecular circadian mechanism. In *Clock* mutant mice, the expression of other clock genes is disrupted, with reduced peak expression of each gene[10–12], and reduced photoreception[13]. Scheer et al.[14] reported that light causes a decrease in T_b via the SCN. Therefore, light appears to be an important factor in inducing torpor-like hypothermia. Although there is controversy as to whether the circadian system remains functional during true torpor in European hamsters[15], our results suggest that *Clock* and/or the normal molecular oscillation of clock genes may be necessary in the induction of torpor-like hypothermia.

cFos expression, a marker for neuron activation[16], was different in the SCN and dSPZ in the dark and light phases during ad-lib feeding in wild-type mice (**Fig. 5e,f**). There were no differences in counts of cFos in other hypothalamic areas. It has been reported that light exerts a strong influence on cFos expression in the SCN[17–19]. However, counts of cFos-IR cells in the light phase were much greater in wild-type mice than in *Clock* mutant mice, perhaps related to lower photoreception in *Clock* mutant mice[13]. Saper et al.[20] reported that the SPZ, which resides just dorsal to the SCN, is a major outflow site from the SCN. Microlesions of the dSPZ resulted in disruption of the circadian T_b rhythm[21]. We found cFos expression in the dSPZ in wild-type mice increased in the dark phase and decreased in the light phase. This is opposite to the results for the SCN (**Fig. 5e,f**), but is consistent with data obtained from

simultaneous neural recordings from the SCN and SPZ[22]. We found no significant phase differences in cFos expression in the dSPZ in *Clock* mutant mice. These results suggest that the functional connections related to T_b between the SCN and dSPZ are not functional in the *Clock* mutant mice.

Fasting affects cFos expression in the SCN both in wild-type and in *Clock* mutant mice, but smaller increases in the counts were detected in *Clock* mutant mice compared with wild-type mice. The increase in cFos-IR cells was not specific to specific subregions of the SCN. In contrast to our results, Liu et al.[7] reported that fasting attenuated cFos expression in the dorsomedial area of the SCN in rats. It is unclear which factor during fasting modulates cFos expression in the SCN, and if there is a difference in the response between rats and mice. However, in ground squirrels (true hibernators), cFos expression in the SCN increased during torpor induced by the cold in constant darkness[23]. Fasting-induced cFos expression in the SCN may also be related to the torpor-like hypothermia observed in wild-type mice.

The number of cFos-IR-labeled cells increased during fasting in other hypothalamic areas in wild-type mice, with a difference between the dark and light phases (**Fig. 5a–d**). There were smaller increases in the DMH, ARC, and PVN in *Clock* mutant mice, but no phase differences were observed. It was reported that neural outputs from the SCN, including the SPZ, reach these areas[24–26]. Thus, activation of the SCN during fasting may be linked with activation of other hypothalamic areas. The MPO is thought to be the integrator of central and peripheral thermal information sent to various brain regions involved in autonomic thermoregulation[27–31]. The sympathetic outflow may originate from the PVN[32–34]. It has been shown that these two nuclei are involved in torpor in hamsters and squirrels[35,36]. The DMH receives thermal input from the skin and the BAT

thermogenesis[30]. Although cFos expression in the hypothalamic areas is involved in functions other than thermoregulatory responses, the changes in cFos expression between the phases may, in part, be responsible for the hypothermia observed in the light phase.

The ARC showed phase differences in cFos expression in wild-type mice (**Fig. 5c**). It has been reported that fasting increased cFos expression in the ARC in mice[37,38]. Although the phase difference in the changes has not been examined, a previous study showed there were more cFos-IR cells in the dark phase than in the light phase during ad-lib feeding[39]. The ARC also receives neural input from the SCN[40–42]. The ARC is involved in regulating food intake and energy expenditure, receiving peripheral nutritional signals such as levels of leptin and insulin[43]. We did not determine if the circulating peptide levels changed between dark and light phases, but the change would have been small during fasting, with the same body weight reductions. We believed that the fasting signals received by the ARC were augmented in the dark phase and attenuated in the light phase in wild-type mice, and this may be related to the signals from the SCN.

Thermoregulation in the cold during ad-lib feeding and fasting

During ad-lib feeding, T_b in the cold was maintained at the level measured at 27°C in both wild-type and *Clock* mutant mice (**Fig. 2a–d**). $\dot{V}O_2$, an index of metabolic heat production, was greater than at 27°C at ZT2.5–3.5 in the light phase in wild-type mice (**Fig. 2e**), and in both phases (ZT3–4 and 13.5–14) in *Clock* mutant mice (**Fig. 2g,h**). The increase in $\dot{V}O_2$ may have been related to spontaneous activity, but only in the dark phase in *Clock* mutant mice (**Fig. 3d**). Therefore, the heat-production response to the cold was activated in the light phase in both mutant and normal mice, suggesting light

was involved. However, even if there was a difference in $\dot{V}O_2$, T_b was the same in normal and mutant mice. In addition, UCP1 mRNA, an indicator of the BAT thermogenesis (nonshivering thermogenesis), was not affected by cold exposure and showed no difference between the two phases (**Fig. 4**) in normal and mutant animals. Therefore, the thermoregulatory responses of heat production at 20°C and the phase differences were small during ad-lib feeding in both groups. It has been reported that cFos expression in the hypothalamus is activated in the cold at 4°C and 10°C[44–46]. However, only a slight increase in cFos expression was observed in the MPO in the light phase in wild-type mice (**Fig. 5a**), so the hypothalamic responses to 20°C cold would also have been small.

In the cold during fasting, there was a large difference in T_b between the dark and light phases in wild-type mice, but no difference was observed in *Clock* mutant mice (**Fig. 2a–d,i**). Metabolic heat production estimated by $\dot{V}O_2$ became greater than that at 27°C in the dark phase in wild-type mice (ZT13.5–14.5, **Fig. 2f**), during which T_b in the two conditions was at the same level (**Fig. 2b**). There was no difference in $\dot{V}O_2$ between the two conditions in the light phase in the wild-type mice (**Fig. 2e**), whereas T_b gradually decreased (**Fig. 2a**). The cold response in *Clock* mutant mice was similar in both the dark and the light phases (**Fig. 2c,d**), at the same level measured in the dark phase in wild-type mice (**Fig. 2i**). The increase in UCP1 mRNA was limited to the dark phase in wild-type mice, but was present in both phases in *Clock* mutant mice (**Fig. 4**). These results clearly show that thermoregulation is different during fasting in the dark and light phases and that *Clock* and/or the molecular circadian mechanism is probably involved. It has been reported in humans that circadian changes in T_b are largely caused by differences in heat loss between night and day[47,48]. Nagashima et al.[6,8] suggested that heat-loss responses in fasted rats and mice determine

T_b and maintain the rhythm in a thermoneutral condition. However, we found that heat-production responses to the cold were also modulated by fasting, a factor that determined changes in T_b.

As summarized in **Table 1**, the increase in cFos expression in *Clock* mutant mice attributable to the cold during fasting was also observed in all the hypothalamic areas except for the SCN, and it was similar in the dark and light phases. In wild-type mice, cFos expression in the SCN was augmented in the light phase. However, the increases in the MPO and PVN in these mice were lower than those observed in *Clock* mutant mice. There have been no studies of cFos expression in the hypothalamus under these conditions. Our results suggest that exposure to cold while fasting increases light-induced neural activity in the SCN only in the presence of *Clock* and/or normal molecular circadian mechanisms. We believe that the attenuated cFos expression in the light phase in the MPO and PVN may result from an inhibitory signal from the SCN. Following cold exposure plus fasting, there was an increase in numbers of neurons in the SCN double-labeled with cFos and CTb injected in the PVN in wild-type mice (**Fig. 6c,d**), whereas counts of double-labeled neurons of cFos and CTb injected in the MPO were unchanged. There were punctate GAD65-IR cells surrounding the double-labeled neurons in the SCN (**Fig. 6g**). The inhibitory role of the PVN in BAT thermogenesis has been reported in rats[49]. Our results indicate that the activation of the PVN may be important in maintaining T_b by facilitating heat-production responses in the cold.

We showed that thermoregulatory responses to the cold differ according to the time of day and feeding conditions. These responses may be important when animals face a reduction in food availability, allowing energy savings without disturbing body temperature during active periods. We demonstrated that the SCN appears to be

important in controlling changes in thermoregulatory responses for the following reasons. First, the activity of the SCN is increased by fasting and cold, for which *Clock* and/or normal molecular circadian mechanisms are required. Second, the metabolic heat response is closely associated with the activity of the SCN. Third, hypothalamic activity during fasting and cold exposure is heavily influenced by the activity of the SCN. We believe that our study is the first to demonstrate that the circadian system not only generates time cues for the circadian T_b rhythm, but also strongly affects thermoregulation itself.

METHODS

Animals. Male *Clock* mutant and wild-type mice (ICR back ground, 2–4 months old, 30–50 g body weight) were used in the present study. They were individually housed in a plastic cage (45 × 25 × 20 cm) with water and food available ad libitum. Ambient temperature (T_a) was maintained at 27 ± 0.5°C, and the lighting cycle set at 12 h light (300 lx at the eye level, lights on at 0700 a.m.) and 12 h complete darkness. The Institutional Animal Care and Use Committee of Waseda University approved all experimental procedures in the present study.

Surgery. A radio transmitter device for the measurement of T_b and spontaneous activity (17 × 10 × 8 mm; Physiotel, model TA10TA-F40, DataScience) was implanted in the abdominal cavity using sterile techniques under inhalation anesthesia with diethyl ether (Sigma Aldrich Japan). Penicillin G (1,000 U, Meiji Pharmaceutical) was injected intramuscularly to minimize postsurgical infection. The mice were allowed to recover for at least 10 d before the experiments.

Experimental protocols. We verified that after surgery mice showed clear circadian T_b and activity rhythms (the rhythms were weak in *Clock* mutant mice). The mice were then deprived of food for 48 h. The mice were divided into four groups with different feeding conditions: food deprivation started at 0900 (ZT2, the light phase trial) or 2100 (ZT14, the dark phase trial), with ad-lib feeding control. Water was available ad libitum throughout the experiments. After fasting for 48 h or ad-lib feeding control, T_a was decreased to 20°C at ZT1–4 (the light phase group) or ZT13–16 (the dark phase group), or kepd at 27°C (thermoneutral control). Each mouse was killed by diethyl-ether inhalation and cervical dislocation. The iBAT was quickly removed for later analysis for uncoupling protein-1 (UCP1) mRNA, the mice were transcardially perfused with 4% paraformaldehyde (PFA) in PBS and the brains

prepared for immunohistochemistry.

Measurements. T_b, $\dot{V}O_2$, and spontaneous activity were measured. The radio-transmitted signals for T_b were sent to a receiver (model CTR86, DataScience) underneath the cage and were stored in a personal computer every 5 min. Spontaneous activity was estimated from the change in the intensity of the telemetry signal. $\dot{V}O_2$ was measured in a half-enclosed Plexiglas metabolic box attached to an airflow system with a constant flow rate of 1500 ml/min. The difference in the oxygen tension between airs in the inlet and that in the outlet was continuously monitored using an electrochemical oxygen analyzer (model LCJ-700, Toray), and the data taken and stored in a personal computer every 15 s. $\dot{V}O_2$ was calculated as the product of the difference in oxygen tension and flow rate divided by the body weight corrected to conditions of standard temperature (0°C), pressure (760 mmHg), and humidity. The weight of each mouse was measured before and after the food deprivation.

UCP1 mRNA analysis. The iBAT sample was immersed in a RNA stabilization reagent (RNA Later, QIAGEN) at 4°C for 12 h and stored at −80°C until extracted. Total RNA was isolated from 0.2–0.4 g of the frozen iBAT sample using an RNA extraction kit for lipid tissues (Rneasy Lipid Tissues Mini Kit, QIAGEN). Briefly, the frozen tissue was homogenized with QIAzol Lysis Reagent® containing phenol plus chloroform (Sigma Aldrich Japan), and the liquid centrifuged at 12,000 × g for 15 min at 4°C after vigorous shaking. Seventy-percent ethanol (Sigma Aldrich Japan) was added to the supernatant, which was centrifuged using a flow-through column. RNase-free water (Ultra Pure Water, Invitrogen Japan) was put on a membrane of the flow-through column, which was centrifuged to elute. The total RNA concentration in the eluent was determined based on the ratio of the absorbance at 260 and 280 nm (NanoDrop ND-1000 spectrophotometer , Thermo Scientific).

Reverse transcription for the total iBAT RNA of 1000 ng was conducted using a reverse transcription kit (PrimeScript RT reagent Kit Perfect Real Time, TAKARABIO). Denaturation was performed at 37°C for 15 min, followed by 85°C for 5 s in a thermal cycler (i Cycler, Bio-Rad Laboratories). To quantify the mRNA level of UCP1, RT-PCR was conducted using an RT-PCR kit (SYBER Premix Ex Taq Perfect Real Time, TAKARABIO). The mRNA level of glyceraldehyde-3-phosphate dehydrogenate (Gapd) was also determined to standardize the UCP1 value. The forward primer for UCP1 cDNA was TACCCAGCTGTGCAATGACCA, and the reverse primer was GCACACAAACATGATGACGTTCC. The forward primer for Gapd cDNA was GGCACAGTCAAGGCTGAGAATG, and the reverse primer was ATGGTGGTGAAGACGCCAGTA. The denaturation protocol was 95°C for 10 s, 95°C for 5 s by 40 cycles, 60°C for 32 min, 95°C for 15 s, 60°C for 20 s, and 95°C for 15 s.

Immunohistochemistry of cFos in the hypothalamic areas. The perfused brain was stored at 4˚C in 4% PFA for 6 h and in 25% sucrose in PBS for another 48 h. Next, 30-μm coronal sections were cut on a cryostat (Microtome Cryostat HM550; Microm International). The sections were treated with 0.3% hydrogen peroxide in PBS in 0.3% Triton X-100 for 30 min and rabbit primary anti-mouse cFos polyclonal IgG (1:15,000, Calbiochem) for 12 h. After rinsing with PBS, the sections were incubated in biotinylated donkey anti-rabbit IgG (1:1,000, Jackson ImmunoResearch) for 90 min, avidin–biotin complex (1:400, Vector Elite Kit) for another 60 min, and then 5% diaminobenzidine tetrahydrochloride (Sigma) in PBS. The sections were mounted on gelatin-coated glass slides and coverslipped. Digital images of the sections were captured (Digital Camera HC 2500 3CCD, Fujifilm), and cFos-IR cells in the MPO, DMH, ARC, PVN, dSPZ, and SCN were counted in three consecutive sections and the

averages calculated. The atlas of Paxinos and Franklin[50] was used to define the position of labeled cells.

CTb injection and cFos and GAD65 immunofluorecent-histochemistry. The fluorescent retrograde tracer cholera toxin b-subunit (CTb) conjugated to Alexa 488 (Invitrogen, Molecular Probes) was used to trace the projections from the SCN to PVN in *Clock* mutant (n = 3) and wild-type (n = 6) mice. Mice were deeply anesthetized by intraperitoneal injection of pentobarbital sodium (50 mg/kg; Somnopentyl, Kyoritsu Seiyaku) and placed in a stereotaxic instrument for brain surgery. An incision was made in the skin overlying the skull, connective tissue was removed from the surface, and a small hole was drilled to allow accessing to the brain. The CTb was reconstituted by dissolving in 100 μL deionized water to a final concentration of 1% and used to backfill in a glass micropipette (internal tip diameter 10–15 μm). The tip of the micropipette was targeted to the PVN and MPO from a vertical approach, defined by the stereotaxic coordinates: 0.2 mm from the midline, 0.8 mm posterior to the bregma, and 4.6 mm below the skull surface (PVN); 0.2 mm from the midline, 0.2 mm posterior to the bregma, and 5.3 mm below the skull surface (MPO). An iontophoretic injection of CTb was made (+10 μA, 7 s ON, 7 s OFF, 5 min) and the micropipette was left undisturbed for 10 min following injection. The skin incision was sutured and Penicillin G was injected intramuscularly to minimize postsurgical infection.

Animals were returned to individual home cages, and 3 d after the surgery, were deprived of food for 48 h, starting at 0900 (ZT2, light phase). After fasting, T_a was decreased to 20°C from 27°C at ZT1–4. In three of six wild-type mice, the food deprivation and cooling exposure were not conducted, as the control experiment. Each mouse was killed by diethyl ether and cervical dislocation, and transcardially perfused with 4% PFA. The brain was subjected to immunofluorecence histochemistry and

stored at 4°C in 4% PFA for 6 h and 25% sucrose in PBS for another 48 h. Ten-micron-thick coronal sections were cut on a cryostat. The sections were washed in PBS and incubated in rabbit primary anti-mouse cFos polyclonal IgG (1:15,000, Calbiochem) and mouse anti-GAD 65 (1:1,000, Abcam) for 12 h. After rinsing with PBS, the sections were reacted to fluorescent secondary antibodies diluted to 1:400 (Alexa Fluor 635 goat anti-rabbit IgG, Invitrogen, Molecular Probes) and 1:40 (Rhodamine-conjugated goat anti-mouse IgG, Cappel) for 60 min. The sections were mounted on gelatin-coated glass slides and coverslipped. The sections were examined with a confocal laser-scanning microscope (Leica TCS SP2, Leica Microsystems), and the photoimages were taken using Leica LCS Lite software.

Statistical analysis. Differences in the means of T_b, $\dot{V}O_2$, activity, UCP1 mRNA, and counts of cFos-IR positive cells were analyzed by four-way ANOVA [phase (lights on vs. lights off) × feeding condition (ad-lib feeding vs. fasting) × T_a (normal vs. cold) × mouse (mutant vs. wild)]. A post hoc test to identify significant differences at a specific time point was performed using the Newman–Keuls procedure. The null hypothesis was rejected at the level of $P < 0.05$. All values were presented as means ± s.e.m.

REFFERENCES

1. Aschoff, J. Circadian control of body temperature. *J. Therm. Biol.* **8**, 143–147 (1983).
2. Lowrey, P. L. & Takahashi, J. S. Mammalian circadian biology: elucidating genome-wide levels of temporal organization. *Annu. Rev. Genomics Hum. Genet.* **5**, 407–441 (2004).
3. Geiser, F. Metabolic rate and body temperature reduction during hibernation and daily torpor. *Annu. Rev. Physiol.* **66**, 239–274 (2004).
4. Sakurada, S. et al. Autonomic and behavioural thermoregulation in starved rats. *J. Physiol.* **526** Pt 2, 417–424 (2000).
5. Yoda, T. et al. Effects of food deprivation on daily changes in body temperature and behavioral thermoregulation in rats. *Am. J. Physiol. Regul. Integr. Comp. Physiol.* **278**, R134–R139 (2000).
6. Nagashima, K. et al. Effects of fasting on thermoregulatory processes and the daily oscillations in rats. *Am. J. Physiol. Regul. Integr. Comp. Physiol.* **284**, R1486–R1493 (2003).
7. Liu, S. et al. Involvement of the suprachiasmatic nucleus in body temperature modulation by food deprivation in rats. *Brain Res.* **929**, 26–36 (2002).
8. Nagashima, K. et al. The involvement of Cry1 and Cry2 genes in the regulation of the circadian body temperature rhythm in mice. *Am. J. Physiol. Regul. Integr. Comp. Physiol.* **288**, R329–R335 (2005).
9. Vitaterna, M. H. et al. Mutagenesis and mapping of a mouse gene, Clock, essential for circadian behavior. *Science* **264**, 719–725 (1994).
10. Jin, X. et al. A molecular mechanism regulating rhythmic output from the suprachiasmatic circadian clock. *Cell* **96**, 57–68 (1999).

11. Kume, K. et al. mCRY1 and mCRY2 are essential components of the negative limb of the circadian clock feedback loop. *Cell* **98**, 193–205 (1999).
12. Oishi, K., Fukui, H. & Ishida, N. Rhythmic expression of BMAL1 mRNA is altered in Clock mutant mice: differential regulation in the suprachiasmatic nucleus and peripheral tissues. *Biochem. Biophys. Res. Commun.* **268**, 164–171 (2000).
13. Shearman, L. P. & Weaver, D. R. Photic induction of Period gene expression is reduced in Clock mutant mice. *Neuroreport* **10**, 613–618 (1999).
14. Scheer, F. A., Pirovano, C., Van Someren, E. J. & Buijs, R. M. Environmental light and suprachiasmatic nucleus interact in the regulation of body temperature. *Neuroscience* **132**, 465–477 (2005).
15. Revel, F. G. et al. The circadian clock stops ticking during deep hibernation in the European hamster. *Proc. Natl. Acad. Sci. U. S. A.* **104**, 13816–13820 (2007).
16. Sagar, S. M., Sharp, F. R. & Curran, T. Expression of c-fos protein in brain: metabolic mapping at the cellular level. *Science* **240**, 1328–1331 (1988).
17. Aronin, N., Sagar, S. M., Sharp, F. R. & Schwartz, W. J. Light regulates expression of a Fos-related protein in rat suprachiasmatic nuclei. *Proc. Natl. Acad. Sci. U. S. A.* **87**, 5959–5962 (1990).
18. Earnest, D. J., Iadarola, M., Yeh, H. H. & Olschowka, J. A. Photic regulation of c-fos expression in neural components governing the entrainment of circadian rhythms. *Exp. Neurol.* **109**, 353–361 (1990).
19. Kornhauser, J. M., Nelson, D. E., Mayo, K. E. & Takahashi, J. S. Photic and circadian regulation of c-fos gene expression in the hamster suprachiasmatic nucleus. *Neuron* **5**, 127–134 (1990).
20. Saper, C. B., Lu, J., Chou, T. C. & Gooley, J. The hypothalamic integrator for circadian rhythms. *Trends Neurosci.* **28**, 152–157 (2005).

21. Lu, J. et al. Contrasting effects of ibotenate lesions of the paraventricular nucleus and subparaventricular zone on sleep-wake cycle and temperature regulation. *J. Neurosci.* **21**, 4864–4874 (2001).

22. Nakamura, W. et al. In vivo monitoring of circadian timing in freely moving mice. *Curr. Biol.* **18**, 381–385 (2008).

23. Bratincsak, A. et al. Spatial and temporal activation of brain regions in hibernation: c-fos expression during the hibernation bout in thirteen-lined ground squirrel. *J. Comp. Neurol.* **505**, 443–458 (2007).

24. Leak, R. K. & Moore, R. Y. Topographic organization of suprachiasmatic nucleus projection neurons. *J. Comp. Neurol.* **433**, 312–334 (2001).

25. Panda, S. & Hogenesch, J. B. It's all in the timing: many clocks, many outputs. *J. Biol. Rhythms* **19**, 374–387 (2004).

26. Kalsbeek, A. et al. SCN outputs and the hypothalamic balance of life. *J. Biol. Rhythms* **21**, 458–469 (2006).

27. Hammel, H. T. Regulation of internal body temperature. *Annu. Rev. Physiol.* **30**, 641–710 (1968).

28. Boulant, J. A. & Hardy, J. D. The effect of spinal and skin temperatures on the firing rate and thermosensitivity of preoptic neurones. *J. Physiol.* **240**, 639–660 (1974).

29. Nagashima, K., Nakai, S., Tanaka, M. & Kanosue, K. Neuronal circuitries involved in thermoregulation. *Auton. Neurosci.* **85**, 18–25 (2000).

30. Nakamura, K. & Morrison, S. F. Central efferent pathways mediating skin cooling-evoked sympathetic thermogenesis in brown adipose tissue. *Am. J. Physiol. Regul. Integr. Comp. Physiol.* **292**, R127–R136 (2007).

31. Romanovsky, A. A. Thermoregulation: some concepts have changed. Functional architecture of the thermoregulatory system. *Am. J. Physiol. Regul. Integr. Comp.*

Physiol. **292**, R37–R46 (2007).

32. Freeman, P. H. & Wellman, P. J. Brown adipose tissue thermogenesis induced by low level electrical stimulation of hypothalamus in rats. *Brain Res. Bull.* **18**, 7–11 (1987).
33. Amir, S. Stimulation of the paraventricular nucleus with glutamate activates interscapular brown adipose tissue thermogenesis in rats. *Brain Res.* **508**, 152–155 (1990).
34. Yoshimatsu, H., Egawa, M. & Bray, G. A. Sympathetic nerve activity after discrete hypothalamic injections of L-glutamate. *Brain Res.* **601**, 121–128 (1993).
35. Satinoff, E. Disruption of hibernation caused by hypothalamic lesions. *Science* **155**, 1031–1033 (1967).
36. Ruby, N. F. Paraventricular nucleus ablation disrupts daily torpor in Siberian hamsters. *Brain Res. Bull.* **37**, 193–198 (1995).
37. Wang, L., Martinez, V., Barrachina, M. D. & Tache, Y. Fos expression in the brain induced by peripheral injection of CCK or leptin plus CCK in fasted lean mice. *Brain Res.* **791**, 157–166 (1998).
38. Morikawa, Y., Ueyama, E. & Senba, E. Fasting-induced activation of mitogen-activated protein kinases (ERK/p38) in the mouse hypothalamus. *J. Neuroendocrinol.* **16**, 105–112 (2004).
39. Jamali, K. A. & Tramu, G. Control of rat hypothalamic pro-opiomelanocortin neurons by a circadian clock that is entrained by the daily light-off signal. *Neuroscience* **93**, 1051–1061 (1999).
40. Horvath, T. L. Suprachiasmatic efferents avoid phenestrated capillaries but innervate neuroendocrine cells, including those producing dopamine. *Endocrinology* **138**, 1312–1320 (1997).

41. Saeb-Parsy, K. et al. Neural connections of hypothalamic neuroendocrine nuclei in the rat. *J. Neuroendocrinol.* **12**, 635–648 (2000).

42. Yi, C. X. et al. Ventromedial arcuate nucleus communicates peripheral metabolic information to the suprachiasmatic nucleus. *Endocrinology* **147**, 283–294 (2006).

43. Morton, G. J., Cummings, D. E., Baskin, D. G., Barsh, G. S. & Schwartz, M. W. Central nervous system control of food intake and body weight. *Nature* **443**, 289–295 (2006).

44. McKitrick, D. J. Expression of fos in the hypothalamus of rats exposed to warm and cold temperatures. *Brain Res. Bull.* **53**, 307–315 (2000).

45. Bachtell, R. K., Tsivkovskaia, N. O. & Ryabinin, A. E. Identification of temperature-sensitive neural circuits in mice using c-Fos expression mapping. *Brain Res.* **960**, 157–164 (2003).

46. Bratincsak, A. & Palkovits, M. Activation of brain areas in rat following warm and cold ambient exposure. *Neuroscience* **127**, 385–397 (2004).

47. Smolander, J., Harma, M., Lindqvist, A., Kolari, P. & Laitinen, L. A. Circadian variation in peripheral blood flow in relation to core temperature at rest. *Eur. J. Appl. Physiol. Occup. Physiol.* **67**, 192–196 (1993).

48. Krauchi, K. & Wirz-Justice, A. Circadian rhythm of heat production, heart rate, and skin and core temperature under unmasking conditions in men. *Am. J. Physiol.* **267**, R819–R829 (1994).

49. Madden, C. J. & Morrison, S. F. Neurons in the paraventricular nucleus of the hypothalamus inhibit sympathetic outflow to brown adipose tissue. *Am. J. Physiol. Regul. Integr. Comp. Physiol.* **296**, R831–R843 (2009).

50. Paxinos, G. & Franklin, K. B. J. The Mouse Brain in Stereotaxic Coordinates. Academic Press, New York, USA, (2001).

FIGURE LEGENDS

Figure 1 Typical examples of circadian changes in body temperature (T_b), oxygen consumption rate ($\dot{V}O_2$), and spontaneous activity during ad-lib feeding and fasting in the wild-type and *Clock* mutant mice at 27°C. The x-axis indicates Zeitgeber time (ZT); the lighting condition is shown at the bottom with the open bar denoting the light phase and closed bar the dark phase. Data were plotted in 5-min bins. The vertical dashed line shows the time when the 48-h fasting period was started.

Figure 2 Body temperature (T_b) and oxygen consumption rate ($\dot{V}O_2$) at 27°C or 20°C cold exposure with ad-lib feeding or fasting in the wild-type and *Clock* mutant mice. T_b during fasting decreased in the cold (gray bar, ZT1–4 and ZT13–16) in both the wild-type and the *Clock* mutant mice (**a**). In the ad-lib feeding condition, T_b remained unchanged in the cold. During fasting, $\dot{V}O_2$ in the cold was increased only in the dark phase in the wild-type mice (**e,f**) and in both the dark and the light phases in *Clock* mutant mice (**g**,**h**). Changes in T_b and $\dot{V}O_2$ from the pre-cooling values with fasting and cold are summarized in **i and j**, respectively (time 0 denotes either ZT1 or 13). Values given are the means ± s.e.m. (n = 8). **P* < 0.05, 20°C-cold versus 27°C-control in each feeding condition; #*P* < 0.05, versus dark phase in wild-type and both phases in *Clock* mutant mice; §*P* < 0.05, versus dark phase in wild-type and light phase in *Clock* mutant mice.

Figure 3 Spontaneous activity during exposure to 20°C cold or 27°C under ad-lib feeding (**a**–**d**) or fasting (**e**–**h**) in wild-type and *Clock* mutant mice. In *Clock* mutant mice, activity was increased at 20°C (gray bars, ZT1–4 and ZT13–16) only in the dark phase in both feeding conditions (**d,h**). Values are means ± s.e.m. (n = 8). **P* < 0.05,

20°C-cold versus 27°C-control.

Figure 4 The levels of uncoupling protein-1 (UCP1) mRNA in the interscapular brown adipose tissue after 20°C or 27°C exposure with ad-lib feeding or fasting in wild-type and *Clock* mutant mice. The UCP1 mRNA level was expressed in arbitrary units (a.u.), divided by the mRNA level of glyceraldehyde-3-phosphate dehydrogenate. During fasting, UCP1 mRNA increased in the cold compared with the 27°C control (con) in the dark phase in the wild-type mice and in both the dark and light phases in the *Clock* mutant mice. Values are means ± s.e.m (n = 5–8). §$P < 0.05$, 20°C-cold versus 27°C-control; †$P < 0.05$, fasted versus ad-lib fed; #$P < 0.05$, wild-type versus *Clock* mutant mice.

Figure 5 Counts of cFos-immunoreactive cells in the medial preoptic nucleus (MPO; **a**), dorsomedial hypothalamus (DMH; **b**), arcuate nucleus (ARC, **c**), paraventricular nucleus (PVN; **d**), dorsal subparaventricular zone (dSPZ; **e**), and suprachiasmatic nucleus (SCN; **f**) under various conditions. Values are means ± s.e.m (n = 8). *$P < 0.05$, dark versus light phase; §$P < 0.05$, 20°C-cold versus 27°C-control; †$P < 0.05$, fasted versus ad-lib fed; #$P < 0.05$, wild-type versus *Clock* mutant mice.

Figure 6 Immunofluorescence photomicrographs of the dorsomedial (**a,c,e**) and ventrolateral (**b,d,f**) regions of the suprachiasmatic nucleus (SCN) showing the distribution of cholera toxin b-subunit (CTb, green) and cFos (blue) during 27°C exposure with ad-lib feeding (**a,b**) and 20°C cold exposure with fasting (**c,d**) in wild-type mice and in the cold with fasting in *Clock* mutant mice (**e,f**). Arrows indicate cells the double-labeled with CTb and cFos. **g** shows high-magnification

photomicrographs of triple-labeled neurons containing CTb (green), cFos (blue), and GAD65 (red) in the SCN in fasting wild-type mice. Scale bar is 50 μm in **a**–**f** and 15 μm in **g**.

ACKNOWLEDGMENTS

The present study was supported partly by KAKENHI No. 17390062 and 20790195 from the Japan Society for the Promotion of Science, and Project Research of the Advanced Research Center for Human Sciences and Academic Frontier Center, Waseda University.

AUTHOR CONTRIBUTIONS

K.T. and Y.U carried out the experiments and analyzed the data. K.T. and K.N. contributed to the experimental design and wrote the manuscript.

Table 1 Summary of cFos-immunoreactive cells in each hypothalamic nucleus and thermoregulatory responses at 20°C with fasting

	Wild-type		*Clock* mutant	
Nucleus	Light	Dark	Light	Dark
MPO	↑	↑↑↑	↑↑	↑↑
DMH	↑↑	↑↑↑	↑↑	↑↑
ARC	↑↑	↑↑↑	↑↑	↑↑
PVN	↑	↑↑↑	↑↑	↑↑
dSPZ	↑↑	↑↑↑	↑↑	↑↑
SCN	↑↑↑	–	↑	–
Thermoregulatory				
T_b	↓↓↓	↓	↓	↓
$\dot{V}O_2$	–	↑	↑	↑↑
iBAT UCP1	–	↑	↑↑	↑↑

Relative change of cFos-immunoreactive cells in the hypothalamic areas and thermoregulatory changes were shown. ↑denotes “increase”, ↓ and “decrease”. – indicates no significant change. MPO, medial preoptic nucleus; DMH, dorsomedial hypothalamus; ARC, arcuate nucleus; PVN, paraventricular nucleus; dSPZ, dorsal subparaventricular zone; SCN, suprachiasmatic nucleus; T_b, body temperature; $\dot{V}O_2$, oxygen consumption rate; and iBAT UCP1, mRNA level of uncoupling protein-1 in the interscapular brown adipose tissue.

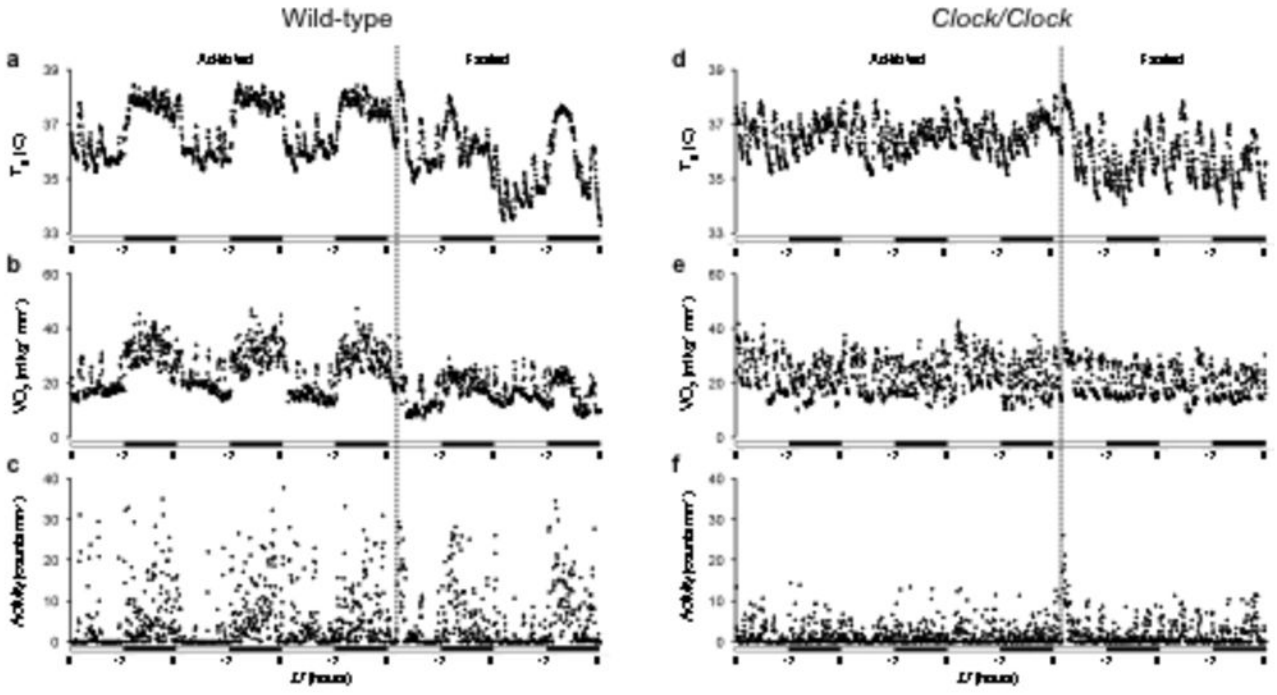

Fig. 1

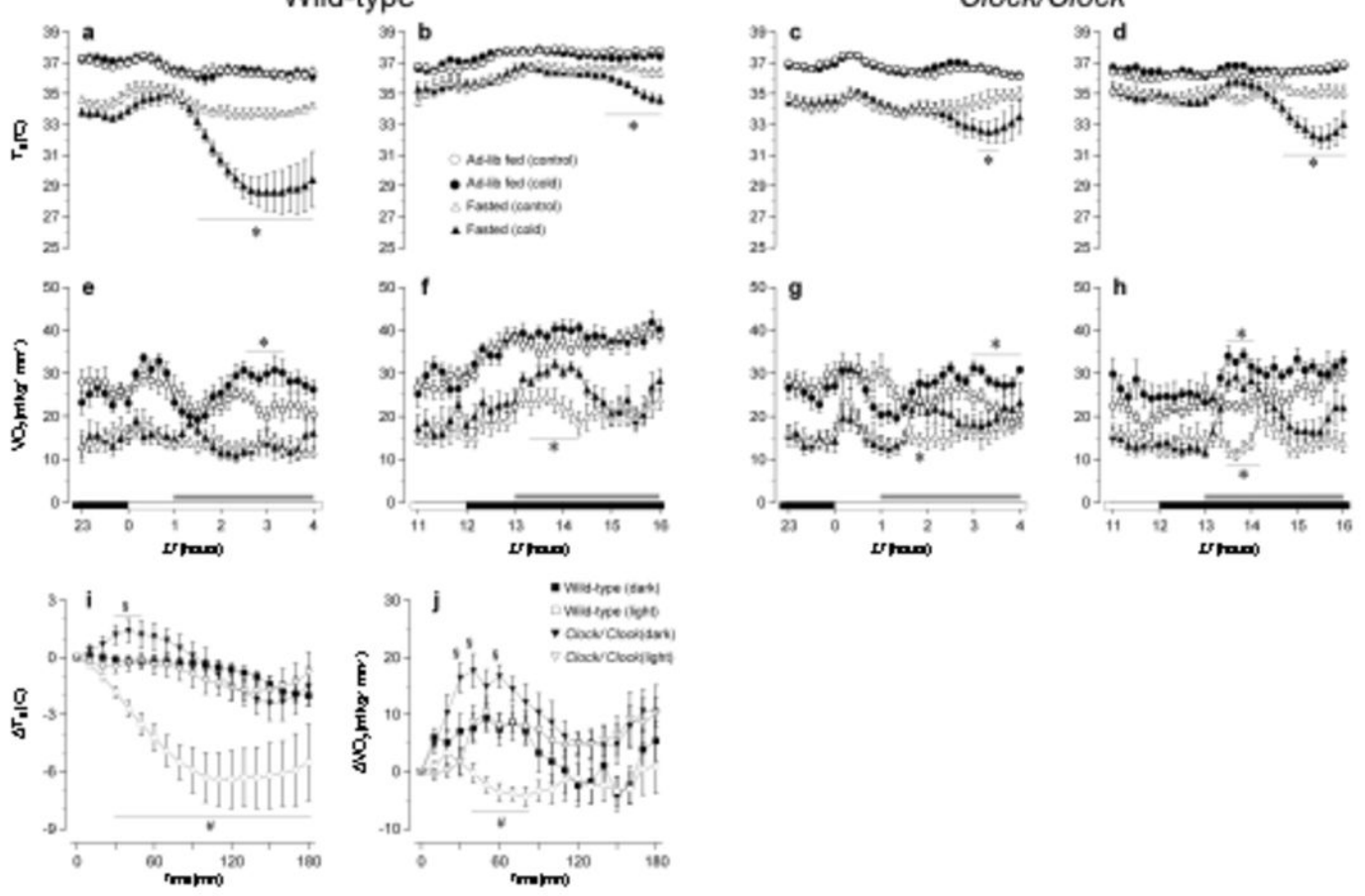
Wild-type
Clock/Clock
a
b
c
d
e
f
g
h
i
j
Ad-lib fed (control)
Ad-lib fed (cold)
Fasted (control)
Fasted (cold)
Wild-type (dark)
Wild-type (light)
Clock/Clock(dark)
Clock/Clock(light)
LT (hour)
Time (min)

Fig. 2

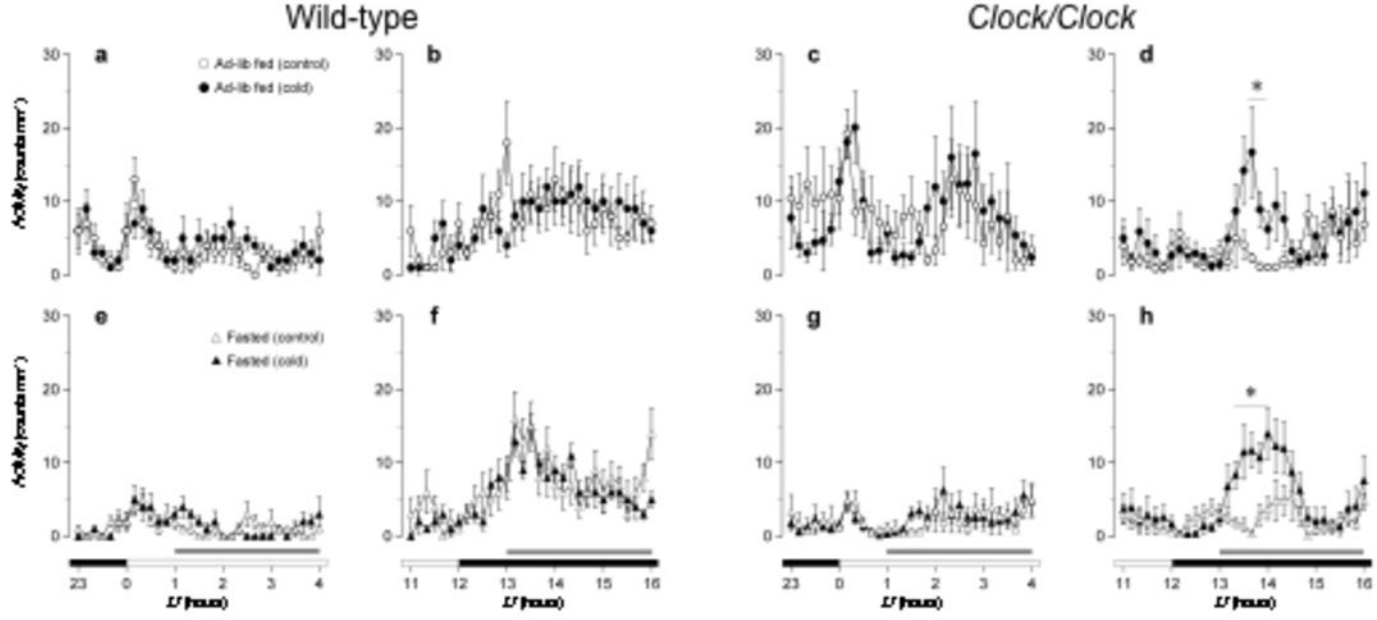
Wild-type
Clock/Clock
a
b
c
d
e
f
g
h
Ad-lib fed (control)
Ad-lib fed (cold)
Fasted (control)
Fasted (cold)
*
*
LT (hour)

Fig. 3

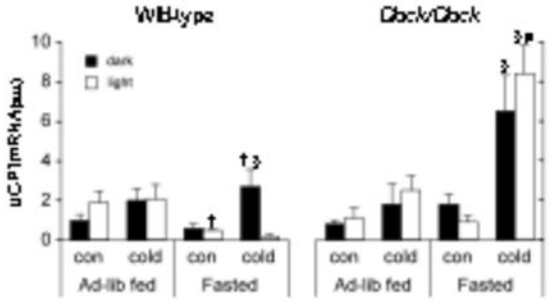
WT/type
Clock/Clock
dark
light
10
8
6
4
2
0
con
cold
con
cold
Ad-lib fed
Fasted
con
cold
con
cold
Ad-lib fed
Fasted

Fig. 4

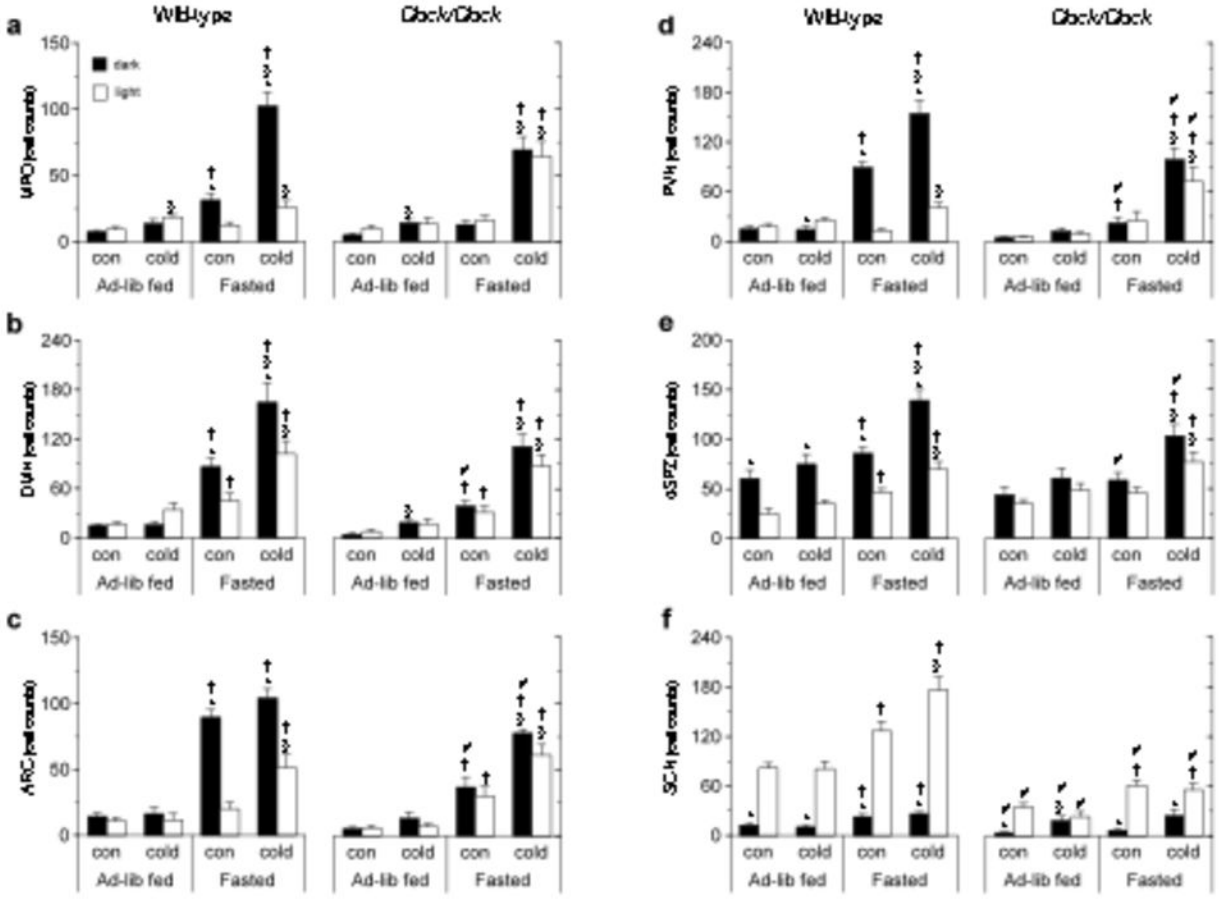
a
b
c
d
e
f
Wild-type
Clock/Clock
dark
light
con
cold
Ad-lib fed
Fasted

Fig.5

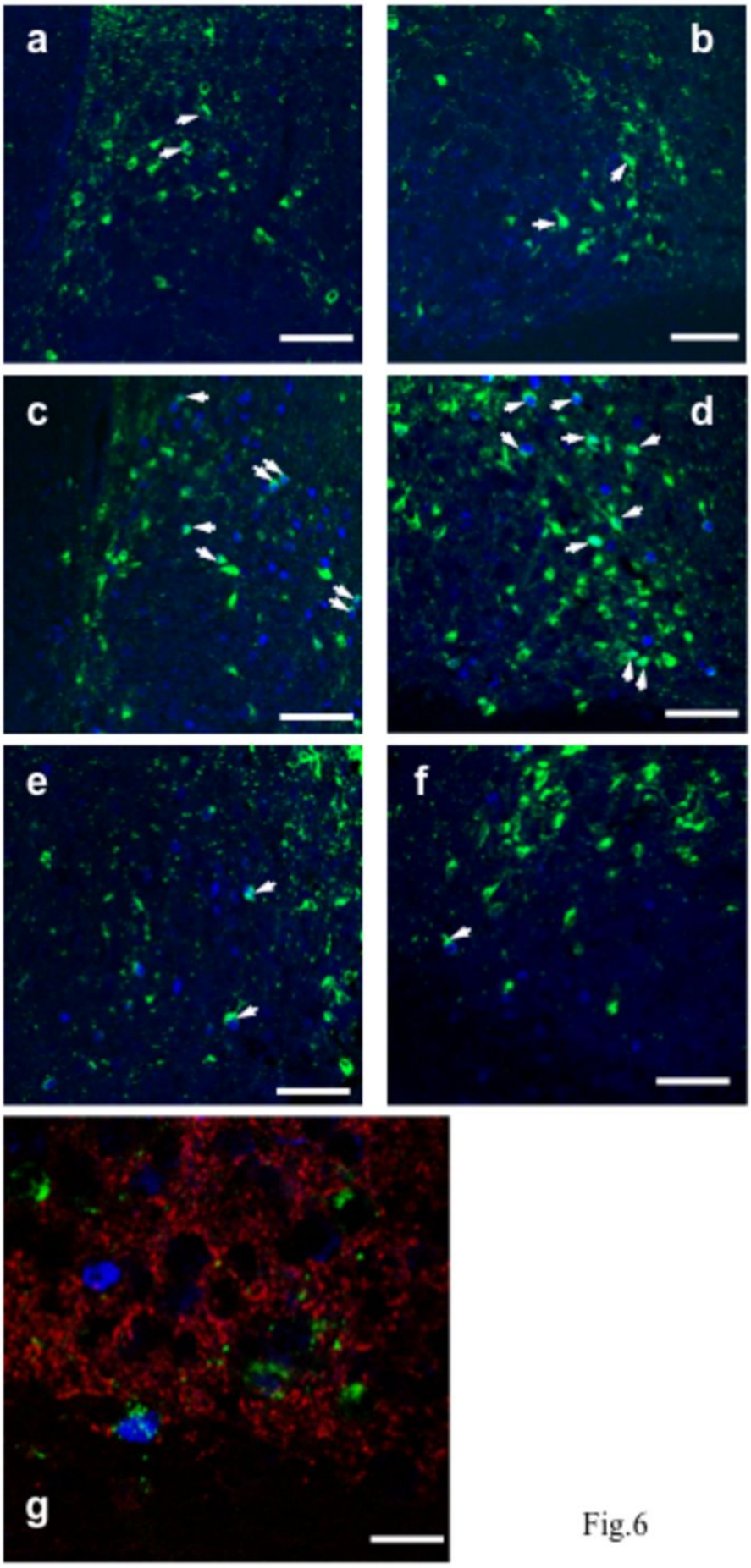

Fig.6